Reviews and syntheses: Opportunities for robust use of peak intensities from high resolution mass spectrometry in organic matter studies

William Kew[1], Allison Myers-Pigg[2], Christine H. Chang[2], Sean M. Colby[2], Josie Eder[1], Malak M. Tfaily[3], Jeffrey Hawkes[4], Rosalie K. Chu[1], James C. Stegen[2,5*]

[1]Environmental Molecular Sciences Laboratory, Richland, WA 99352, USA
[2]Pacific Northwest National Laboratory, Richland, WA 99352, USA
[3]Department of Environmental Science, University of Arizona, Tucson, AZ, 85719, USA
[4]Department of Chemistry, University of Uppsala, Uppsala, 75124, Sweden
[5]School of the Environment, Washington State University, Pullman, WA, 99164,USA

*Correspondence to: James C. Stegen (James.Stegen@pnnl.gov)

Abstract Earth's biogeochemical cycles are intimately tied to the biotic and abiotic processing of organic matter (OM). Spatial and temporal variation in OM chemistry is often studied using direct infusion, high resolution Fourier transform mass spectrometry (FTMS). An increasingly common approach is to use ecological metrics (e.g., within-sample diversity) to summarize high-dimensional FTMS data, notably Fourier transform ion cyclotron resonance MS (FTICR MS). However, problems can arise when FTMS peak intensity data are used in a way that is analogous to abundances in ecological analyses (e.g., species abundance distributions). Using peak intensity data in this way requires the assumption that intensities act as direct proxies for concentrations. Here we show that comparisons of the same peak across samples (within-peak) may carry information regarding variation in relative concentration, but comparing different peaks (between-peak) within or between samples does not. We further developed a simulation model to study the quantitative implications of using peak intensities to compute ecological metrics that rely on information about both within-peak and between-peak shifts in relative abundance. We found that despite analytical limitations of linking concentration to intensity, the ecological metrics often perform well in terms of providing robust qualitative inferences and sometimes quantitatively-accurate estimates of diversity and molecular characteristics. We conclude with recommendations for robust use of peak intensities for natural organic matter studies. A primary recommendation is the use and extension of the simulation model to provide objective guidance on the degree to which conceptual and quantitative inferences can be made for a given analysis of a given dataset. Broad use of this approach can help ensure rigorous scientific outcomes from the use of FTMS peak intensities in environmental applications.

1 Introduction

Organic matter (OM) plays a central role in Earth's biogeochemical cycles, and is both a resource for and product of metabolism. The detailed chemistry of OM (e.g., nominal oxidation state) can modulate and reflect biogeochemical rates and fluxes within and across ecosystems (e.g., LaRowe and Van Cappellen, 2011; Boye et al., 2017; Garayburu-Caruso et al., 2020), yet our understanding of this complexity is limited by our analytical abilities to view it (Steen et al., 2020; Hedges et al., 2000; Hawkes and Kew, 2020a). Given the importance of OM chemistry to biogeochemical cycling, there is a need to understand how and why that chemistry varies through space and time. To help meet this need, there has been growing interest in using concepts and methods from ecology to study the chemogeography and chemodiversity of OM in a variety of ecosystems (e.g., Kujawinski et al., 2009; Kellerman et al., 2014; Tanentzap et al., 2019; Danczak et al., 2021). This is a promising approach as there are many conceptual

parallels between the chemical species that comprise OM and the biological species that comprise ecological communities (Danczak et al., 2020).

The most fundamental ecological data type is the species-by-site matrix. This matrix indicates how many individuals of each species occur in each sampled community. Ecologists use species-by-site matrices to ask myriad questions related to biological diversity. Two common analyses are known as α-diversity and β-diversity, each with numerous metrics (Whittaker, 1972; Anderson et al., 2011). α-diversity measures the diversity within a given community. β-diversity has been variously defined, but essentially measures variation in composition across communities. Both α-diversity and β-diversity can be quantified using presence-absence data or they can include estimates of each species' relative abundance within and between communities (Fig. 1).

The chemistry of OM is commonly studied using high resolution Fourier transform mass spectrometry (FTMS) techniques (e.g., Hawkes and Kew, 2020b), such as Orbitrap or Ion Cyclotron Resonance (ICR) MS, via direct infusion of samples. At present, the highest resolution approach for untargeted analysis of OM is via a 21 Tesla FTICR MS (Marshall et al., 1998; Shaw et al., 2016; Smith et al., 2018; Bahureksa et al., 2021). The output data produced is a spectrum containing peaks represented by a signal intensity (Fig. 2 y-axis) and a mass-to-charge ratio (*m/z*) (Fig. 2 x-axis), which is equivalent to the mass for singly charged ions as routinely detected in natural organic matter (NOM) measurements. In turn, regardless of the type of MS instrument used, the MS data inherently lead to an OM peak-by-sample data matrix, akin to an ecological species-by-site data matrix. The high resolution data from MS often results in a large matrix, wherein a single sample may contain thousands to tens of thousands of peaks. To take advantage of these rich data, FTMS data have been analyzed using the same α-diversity and β-diversity metrics that are commonly used by ecologists to study biological diversity (e.g., Kellerman et al., 2014). Such analyses are exciting, as they enable the same conceptual questions and quantitative frameworks to be applied to biological (e.g., microbial communities) and chemical (i.e., OM) components that directly interact with each other within ecosystems (Lucas et al., 2016; Osterholz et al., 2016; Li et al., 2018; Tanentzap et al., 2019; Danczak et al., 2020, 2021).

The use of ecological metrics with MS data is particularly common with FTMS datasets and there is great potential to continue leveraging concepts from ecology in high-resolution OM analyses. Care is required, however, in using FTMS peak intensity data to estimate α-diversity, β-diversity, and related ecological analyses (e.g., 'species' abundance distributions). Key to these ecological analyses is the assumption that within complex NOM samples, differences in peak intensity are proportional to differences in concentrations of the associated molecules. Studies using FTMS often avoid using peak intensities due to uncertainties in whether it is valid to assume proportionality between peak intensities and concentrations within and across NOM samples (Kujawinski, 2002). These studies may be discarding useful information, though it is unclear what biases and uncertainties are introduced into ecological metrics when using FTMS peak intensities. To help advance robust use of FTMS datasets for NOM studies, we review the theoretical reasons why peak intensities may not reflect true concentrations, provide empirical evaluation of this theory, and invoke *in silico* simulation to quantify the associated impacts on ecological analyses. While theory and empirical analyses demonstrate disconnects between peak intensities and concentrations in FTMS data, the simulations show that ecological metrics are often still robust. We end with practical recommendations and propose a path forward for increasing robust use of FTMS peak intensities for NOM studies.

2 Theoretical Foundations

Here we provide a review of the theoretical foundations behind why assuming proportionality between peak intensities and concentrations in FTMS can be challenging. This section will be of most value to FTMS data users that are not formally trained in mass spectrometry, and serves as a review of mass spectrometry principles (see also Kujawinski, 2002; Urban, 2016; Bahureksa et al., 2021). We focus on FTMS (i.e., FTICR and Orbitrap), but many of the principles are applicable across all MS platforms. We highlight three considerations: ionization, ion transfer, and ion signal detection in the context of commercial FTMS instruments. These considerations have practical

implications tied to within-peak and between-peak comparisons (Fig. 2). Here, we define 'within-peak' as comparing peak intensities of the same feature (i.e., *m/z* or molecular formula) across different sample spectra and 'between-peak' as comparing peak intensities across different features. As discussed below, within-peak comparisons can be robust under certain situations, but there are limitations with between-peak comparisons that may be unavoidable. The following discussion is not an exhaustive treatment of all decisions associated with a complete FTMS experiment, and we do not deeply address factors such as sample preparation, choice of ionization mode, and instrument specific parameter optimization. These topics have been discussed in a recent review (Bahureksa et al., 2021).

2.1 Ionization Efficiency and Isomers

Electrospray ionization (ESI) is the most common technique for generating ions from NOM samples. When using ESI, the peak intensity for any given molecular mass (or molecular formula) will depend on both concentration and ionization efficiency, the latter of which is dependent on structure, pKa, and the other molecules in the sample (Kruve et al., 2014). In NOM samples, one detected mass or peak combines signals from multiple isomers which all have the same molecular formula but different structures. The different structures impact ionization efficiency, but FTMS data contains no information about this structural variation. Unfortunately, to date, no liquid chromatography (Kim et al., 2019; Han et al., 2021) or ion mobility separation (Tose et al., 2018; Leyva et al., 2020) technique has yet demonstrated sufficient resolution to completely infer structural variation among isomers within complex NOM samples. Unknown variation in structure can, therefore, lead to unknown variation in peak intensities. This challenge can be compounded by ionization suppression that occurs when the ionization efficiency of one type of molecule (i.e., peak) is altered by the presence of other types of molecules (Ruddy et al., 2018). Ionization suppression can be mitigated by online separation whereby non-targeted LC-MS approaches may yield more quantitative data (Kruve, 2020), but matrix effects remain a significant issue even for LC-MS (Trufelli et al., 2011). In NOM samples with thousands of types of organic molecules, the molecular interactions likely have complex influences over realized ionization efficiencies. While it is possible to control for some of these challenges (e.g., using consistent sample concentrations and preparations), many additional factors (e.g. molecular structures, pKas, and interactions among molecules in NOM samples) cannot yet be accounted for. Interpretation of peak intensities as proxies for concentrations in FTMS datastreams may, therefore, be prone to uncertainty.

2.2 Ion transmission and collection

In FTMS, packets of ions are accumulated in a trap prior to their transmission to the analyzer cell (Fig. 3 Panel A section d; Senko et al., 1997; Makarov et al., 2006). The duration of time in which ions are accumulated is often varied to yield an optimal ion population for the analyzer cell. The duration of this event can change the relative abundance, and thus observed peak intensities of different ions (Cao et al., 2016). Increases in the true abundance of other ions can decrease the measured peak intensity of a given ion due to a dilution effect resulting from a finite number of ions that can fit within the ion trap. Additional challenges arise due to variation in the speed at which different ions move from the accumulation trap and into the analysis cell. Smaller ions move more quickly and therefore reach the analysis cell sooner than larger ions. Variation in the accumulation time across samples and FTMS instruments, combined with among-ion variation in transmission speed, can introduce additional uncertainty in the relationship between peak intensities and true concentrations.

2.3 Ion signal detection

The final step in data collection via FTMS is signal detection. The intensity of the signal is proportional to the abundance of a given ion in the analysis cell, the proximity of ions to the detector (Kaiser et al., 2013), and the ion charge state (Wörner et al., 2020). Similar to molecular interactions impacting ionization efficiencies, different types of ions can interact to affect each other's signal intensity. The Fourier transform applied to the data also complicates extremely accurate relative quantification of ion abundance between peaks (Makarov et al., 2019). These challenges

at the detection stage can add more uncertainty to the relationship between peak intensity and concentrations, particularly for complex NOM samples.

3 Empirical Evaluations

In this section, we move beyond theoretical considerations to empirical evaluations of the real-world relationships between peak intensities and concentrations. Similar to above, this section will be of primary value to those without formal training as mass spectrometrists, but who use FTMS data to study NOM.

3.1 Direct comparison of peak intensities in idealized samples

As discussed above, different organic compounds ionize with different efficiencies. In theory, this may lead to variation in observed peak intensities even when all organic compounds have the same true concentration. To evaluate this theoretical expectation, we analyzed several different types of organic compounds in different conditions via FTICR-MS. We selected chemical standards which are natural products with molecular formula and chemistries typical of compounds commonly observed in organic matter, and were amenable to negative mode ESI analysis. First, we analyzed three separate dilution ladders of individual pure compounds dissolved in pure methanol. These standards were analyzed at higher concentrations than typically observed for NOM because they were single compounds rather than formula-summed features (with multiple isomers) within a NOM spectrum; higher concentrations were required to compensate for lower isomeric diversity. These three compounds gave rise to different peak intensities under otherwise identical conditions (Fig. 4A). Trehalose, for example, had much lower peak intensity than sinapic acid at the same actual concentration. The difference in signal intensity was also apparent amongst compounds that ionize well under negative mode ESI; for example, two different structures containing the same number of carboxylic acid units exhibited differences in signal intensity. We also observed differences in peak intensities amongst structural isomers (i.e., same molecular formula and mass) (Fig 4B). Each peak observed via direct infusion FTICR-MS may be several isomers. These isomers may be observable through chromatographic separation (Kim et al., 2019), ion mobility separations (Leyva et al., 2019), or by statistical inference of tandem mass spectrometry (Zark et al., 2017), but not via direct infusion FTICR-MS. We note that absolute differences in signal intensity may be smaller between molecules at lower concentrations, but this does not necessarily mean that low intensity signals consistently indicate low concentrations and this does not aid in quantitatively interpreting higher intensity signals. In summary, differences in peak intensities across organic compounds do not necessarily equate to differences in concentration, unless assessed via a calibration curve for each compound.

3.2 Comparison of peak intensities in in real world samples

Routine NOM samples contain a diverse range of thousands of molecules of unknown structures and relative concentrations and often contain inorganic interferences, such as salts. Sample clean up that focuses on pre-concentration and desalting is imperfect (Raeke et al., 2016; Li et al., 2017), but is commonly used to minimize inorganic interferences. Interactions among molecules remains a challenge, however, as discussed above. The collection of molecules in a sample is referred to here as the 'matrix.' To explore matrix effects on peak intensities, we prepared solutions of six different pure compounds at a fixed concentration (100 ppb) in three different solvent systems - pure methanol, methanol eluted from a BondElut SPE cartridge, and methanol from elution off of a BondElut SPE cartridge which had been loaded with artificial river water (ARW). Additionally, we added a complex mixture that is often used as a NOM standard, Suwannee River Fulvic Acid (SRFA), at six different concentrations, to each sample. Samples were analyzed independently but contemporaneously on the same instrument to mirror a real study.

In methanol-only solvent, with no added SRFA, the six compounds yielded different peak intensities (Fig. 4C), which is consistent with results from the previous subsection. As the concentration of SRFA was increased to 2

ppm, the relative signal intensity increased for some of the six compounds, but decreased for others. Above 2 ppm of SRFA, peak intensities for all six compounds were substantially decreased. Use of an 'impure' methanol solvent, i.e., the eluent from a SPE blank (Fig. 4D) or from an SPE of artificial river water (Fig. 4E), resulted in further decreases in peak intensities. In both cases, the maximum peak intensity was ~20% of what was seen in pure methanol (Fig. 4C), and some of the six compounds were no longer observed. Addition of SRFA to these samples with 'impure' solvents, again, generally, decreased peak intensities.

Combining the empirical results from this subsection and the previous subsection with instrument theory discussed above suggests significant uncertainty in relationships between true concentrations and peak intensities from direct infusion FTICR-MS. Calibration curves can be used in the simplest of situations, but may be challenging when there are structural isomers and sample-to-sample variation in matrix composition. Modeling of constrained systems may, however, allow for data-driven and mechanistic data normalization strategies for enhanced use of peak intensity data.

4 Conceptual implications for use of ecological metrics

The preceding sections indicate challenges when using FTMS peak intensities as proxies for relative changes in concentrations of organic molecules. The implication is that some ecologically-inspired analyses (e.g., Fig. 1) may be challenging to use with FTMS peak intensity data. To understand which analyses could be impacted, we differentiate analyses into two classes: those based on within-peak intensity comparisons and those based on between-peak intensity comparisons (Fig. 2). As noted above, within-peak is based on comparing the same feature (*m/z* or molecular formula) across spectra/samples, whereas between-peak compares different features (*m/z* or molecular formulas) across and within spectra/samples.

We posit that analyses using FTMS between-peak intensity comparisons could have the greatest uncertainty. Consider an ecological setting in which a researcher aims to quantify within-sample diversity (α-diversity) and among-sample diversity (β-diversity) (Fig. 1) of tree communities (Fig. 5, left side). The researcher will likely set up a plot of a given size and then directly count the number of each tree species in each plot, thus generating the species-by-site matrix filled with directly observed abundance counts for each species. The ability of the researcher to observe individuals of each species does not vary appreciably across species because each tree is not moving and our ability to see a static object is not influenced by environmental factors. Thus, the number of individuals observed for a given tree species is quantitatively comparable to the number of individuals observed for all other tree species in the plot. The assumption that differences in observed abundances carry robust information about differences in actual abundances is thus supported, in this example. In turn, it is valid to use relative abundances to compute α-diversity such as via Shannon evenness (Elliott et al., 1997; Mouillot and Leprêtre, 1999; Redowan, 2015). Furthermore, because the ability to observe each tree species is the same across communities, it is valid to use relative abundances to compute β-diversity (e.g., via Bray-Curtis; Anderson et al., 2011) or conduct other ecological analyses that use abundance data (e.g., species abundance distributions McGill et al., 2007).

We contrast this tree community example with another ecological setting. Consider a researcher studying bird communities (Fig. 5, right side) that estimated species abundances solely based on the number of times an observer hears the call of a given species. In this case, those species that call more frequently and/or more loudly will be more likely to be heard, and thus an observer will infer a higher abundance even if all species in the community have the same abundance. That is, such a method generates data that may indicate which species are present, but the 'call counts' do not carry reliable information regarding absolute or between-species relative abundances. Follow-on analyses of α-diversity and β-diversity should, therefore, be limited to approaches that use presence/absence data, and species abundance distributions cannot be quantified.

If we continue with the bird community example and assume that the detectability of a given bird species is consistent across sampled locations or times, then it would be appropriate to examine variation in within-species call counts. This within-species analysis is directly analogous to the FTMS within-peak time series analysis in Merder et al. (2021), discussed below. However, if call counts of a given species are suppressed by the presence or abundance of other species, then call counts of a given species may not indicate changes in its abundance. The call count example is directly analogous to influences of the NOM matrix: if the presence/abundance of a given organic molecule modifies the ionization of other molecules, then within-peak changes in intensity may not indicate changes in concentration. In turn, analyses based on within-peak intensity comparisons could lead to error and uncertainty in values of computed ecological metrics, especially if there are significant cross-sample changes in the NOM matrix.

As described in the previous sections, the unique chemistry of every molecule in a NOM sample can influence ionization properties for other molecules in the sample. Thus, FTMS data align with the bird community example rather than the tree community example, with the differing physics of each molecule influencing between-peak differences in peak intensity. Molecules that more readily ionize will produce higher peak intensities, which is akin to bird species with noisier or more numerous calls producing a larger number of call counts that do not accurately represent the underlying population distribution. Similarly, between-peak differences in intensity as observed via FTMS cannot be directly used as a proxy to indicate between-peak differences in concentration.

In contrast to between-peak comparisons, within-peak comparisons examine changes in the relative intensity of a single peak across samples. Such within-peak comparisons may be repeated independently for each peak of interest in a given dataset. For example, Merder et al. (2021) quantified temporal dynamics of individual FTMS peaks and then binned peaks into different groups with characteristic temporal fluctuations. In those analyses, peak intensities were not compared between peaks. Instead, the temporal dynamics of each peak was compared to temporal dynamics of other peaks. The underlying assumption of this type of analysis is that a between-sample increase in the intensity of a given peak can be used as a robust proxy of a between-sample increase in concentration of that peak. Materials presented in the previous sections indicate that this assumption can be met in some instances when using FTMS data. However, great care is required with strong attention paid to assumptions of analysis methods. For example, using Pearson correlation makes the assumption that concentration of a given peak is a *linear* function of changes in its peak intensity. We showed above (Fig. 4) that this assumption is not always valid, even in ideal conditions. Using a Spearman correlation avoids this assumption because it is based on ranks. That is, Spearman correlations (e.g., Kellerman et al., 2014) make the more realistic assumption (for FTMS data) that an increase in concentration of a given peak is reflected as an increase in its peak intensity without assuming any statistical or mathematical form of that relationship.

5 Ecological metrics using peak intensities are often robust

The previous sections highlight challenges in connecting between-peak changes in peak intensity to between-peak changes in abundance (Fig. 4). These challenges violate an assumption of abundance-based ecological analyses: proxies for abundance (e.g., peak intensity) should be proportional to true abundances. However, the quantitative impacts of this situation likely vary across ecological metrics and with study details. There may be certain metrics or situations in which robust inferences can be made despite poor linkages between peak intensities and true abundances. These cases are important to understand, especially given the growing number of publications using peak intensities to compute abundance-based ecological metrics.

To provide initial guidance on best practices for using FTMS peak intensities with ecological metrics, we developed an *in silico* simulation model. This model generates synthetic data, introduces errors that degrade the linkage between peak intensity and true abundance, and computes within-sample (e.g., Shannon diversity) and between-sample (e.g., Bray-Curtis) ecological metrics (Fig. 6). The model allows us to probe how the introduction of each

type of error impacts the relationship between true and observed values. To generate synthetic data, we randomly assigned abundances to either 100 or 1000 peaks. Abundances were sampled with replacement from a Gaussian distribution that varied in mean and standard deviation across synthetic samples and across simulation iterations. Abundances were drawn twice to generate two independent samples per simulation, and the simulation was run 100 times for each number-of-peaks (100 or 1000 peaks per sample; referred to below as 'peak richness'). We varied the Gaussian distributions to generate synthetic samples varying in composition within and across simulations to ensure that the ecological metrics (see below) would vary across simulations. This step was necessary to evaluate metric performance across a broad range of metric values.

We simulated two types of error which can both be representative of variation in ionization efficiency. The goal was to generate synthetic data that mimicked our empirical and theoretical observations that indicate noise in the relationships between observed peak intensities and true abundances. For each type of error and within each iteration of the simulation, the error was introduced 100 times (i.e., 100 error iterations were nested within each sample-generation iteration). The first type of error was designed to diminish the between-peak relationship between observed peak intensity and true abundance. To introduce this error, we multiplied the true abundance of each peak by a random number drawn from a uniform distribution ranging from 0 to 100. The inclusion of 0 indicates situations in which a given peak (i.e., ion) does not ionize well enough to be observed. The results should not be sensitive to the selected range, but as a sensitivity analysis, we also used a distribution of errors ranging from 0 to 8. Our empirical data suggest that this narrower range is appropriate (Fig. 4B), but simulation results were not affected by the selected error range (Supplementary Figs. S3-S8). For each peak we multiplied the same random error by its abundance in each of the two synthetic samples within each iteration. This error-modified abundance of each peak in each synthetic sample was considered to be the observed peak intensity. We recognize that randomized errors do not perfectly reflect real-world variation in ionization efficiency. However, because the true impacts of matrix effects and individual molecular chemistries in complex mixtures are currently not known, the errors introduced in the model are simply used to diminish the relationship between observed peak intensities and true abundances.

Introducing error resulted in a relatively weak relationship between observed peak intensity and true abundance (median R^2 = ~0.5; see black line in Figure 7), with the amount of error increasing with true abundance (Fig. S1). This relationship additionally supports our inclusion of error into the model as a means to simulate relatively weak relationships between observed peak intensity and true abundance. Between-peak differences in observed intensity were also weakly related to between-peak differences in true abundance (Fig. 8A), with a median R^2 of ~0.5 (see blue line in Figure 7). Because the same peak-level error-factor was used across both synthetic samples within a given simulation iteration, the within-peak between-sample differences in observed intensity were relatively strongly correlated to within-peak between-sample differences in true abundance (Fig. 8C), with a median R^2 of ~0.75 (see the gray line in Figure 7). As seen in Figure 8C, the differences collapse when near zero. This phenomenon can be explained by the fact that when two samples have essentially the same peak intensity for a given peak, introducing the same error to that peak in both samples has little influence on the between-sample difference in peak intensity.

The second type of error we introduced represents situations in which ionization efficiency varies across molecules – as in the first type of error – as well as across samples. Molecules may exhibit variations in ionization efficiency across samples due to changes in the composition of organic molecules and/or changes in inorganic solutes in the matrix (see above). To account for these effects, we multiplied the true abundance of each peak by a random number drawn from a uniform distribution ranging from 0 to 100; for sensitivity analysis, we also used an error distribution ranging from 0 to 8, which did not have meaningful influences on the results. For each iteration of the simulation, we introduced errors independently for the two synthetic samples. In this way, the simulated ionization efficiency for a given peak in a given synthetic sample was independent of its ionization efficiency in the other synthetic sample. The error-modified abundance of each peak in each synthetic sample was considered to be the observed peak intensity.

We observed a relatively large influence on observed peak intensities when allowing ionization efficiency to vary across samples. That is, the within-peak between-sample differences in observed intensity were weakly correlated to within-peak between-sample differences in true abundance (Fig. 8C), with a median R^2 of ~0.5 (see the red line in Figure 7). Compared to the same relationship that emerged under the first type of error, our results show a much weaker relationship between peak intensity and true abundance when ionization efficiency varies between samples (compare the gray and red lines in Figure 7). This result is expected, as variations in ionization efficiency add random noise to the within-peak between-sample differences in observed peak intensity. We note that the variation in ionization efficiency is independent between peaks for both the first and second types of error. The between-peak relationship summarized in Figure 7 (blue line) is, therefore, equivalent for both types of error, which is further supported by the strong similarity between Figures 8A and 8B.

To examine how both types of error influence ecological metrics, we used the initial true abundances and the error-modified abundances (i.e., observed peak intensity values) to calculate true and 'observed' values of within-sample Shannon diversity and between-sample Bray-Curtis. We also assigned an arbitrary trait value to each peak and calculated true and observed sample-level mean trait values; the mean values for each sample were weighted by true abundance (true mean) or observed peak intensity (observed mean). This analysis is analogous to the approach commonly used in ecological studies for computing community-level abundance-weighted trait values, such as plant leaf area index or animal body size (Muscarella and Uriarte, 2016). This approach is also commonly used with FTMS data, such as sample-level peak-intensity-weighted values of hydrogen-to-carbon ratios and molecular weight (Roth et al., 2019; Wen et al., 2021). We regressed observed values for Shannon diversity, Bray-Curtis, and mean traits against their true values, and performed this process independently for each level of peak richness.

Relating 'observed' values of each metric to their true values revealed that the patterns observed in peak-intensity-based ecological metrics are actually likely to be qualitatively robust despite the existence of quantitative biases (Figs. 9-11). All three ecological metrics showed monotonic relationships between observed and true values. Uncertainty was lower when samples had 1000 peaks, relative to samples with 100 peaks; in Figures 9-11 all A/B and C/D panels have 100 and 1000 peaks, respectively. We observed monotonic relationships and lower uncertainty with more peaks for both within-sample and between-sample error; in Figures 9-11 all A/C and B/D panels have within-sample and between-sample errors, respectively. For Shannon diversity, observed values were consistently lower than true values, but all observed vs. true relationships were linear (Fig. 9). For Bray-Curtis, inclusion of between-sample error resulted in an overestimation of values and non-linear (but monotonic) relationships between observed and true values (Fig. 10). For mean trait values, we found no systematic quantitative biases, and the relationships between observed and true values were consistently linear (Fig. 11).

The variation in observed values explained by true values (via a linear model) increases rapidly with the number of peaks and sharply asymptotes beyond ~500-1000 peaks per sample (Fig. S2). Sample-to-sample changes in the value of ecological metrics can, therefore, be interpreted with increasing confidence as the number of peaks increases. Qualitative gradients are, therefore, more robust with more peaks. The absolute magnitude of some ecological metrics, however, are shifted away from their true magnitude even when there are large numbers of peaks (e.g., Fig. 10D). Quantitative comparisons from one dataset to another may, therefore, require further simulation-based evaluation. We further caution that the number of peaks needed to reach the asymptote, thereby minimizing error, is likely dataset dependent, and 500-1000 peaks should not be taken as a general rule for real-world datasets. We encourage researchers to complete such simulations using the numbers of peaks present across their own real-world datasets to better understand their ability to make statistical and conceptual inferences.

6 Conclusions and Recommendations

There is increasing interest in using ecological metrics with FTMS data to study NOM chemistry . It is vital that this growing body of work be based on rigorous use of the data. This requires deep understanding of the metrics,

awareness of the data limitations, and careful use of the metrics informed by the data limitations. We suggest that studies using FTMS peak intensities need to include material that directly discusses the data limitations, what peak intensities do and do not represent (e.g., tree-like vs. bird-like data; Fig. 5), and how knowledge of those limitations was used to select specific metrics.

We have provided both theoretical reasoning and empirical observations showing that peak intensities do not necessarily map to concentrations of the associated organic molecules within NOM-like complex mixtures of organic molecules. This is particularly true for between-peak comparisons, and statistical post-hoc normalizations of peak intensity data do not solve this challenge. We caution against using between-peak differences in intensity from FTMS data to make direct inferences related to between-peak differences in abundance or concentration. This has implications for some ecological analyses based directly on variation in species abundances. In particular, estimation of 'species abundance distributions' are likely to be problematic. Analyses that bin peaks into high and low abundance groups based on between-peak differences in concentration are also likely to be problematic. We did not directly evaluate these types of analyses, and we suggest that future work should expand upon the ecological metrics examined here via simulation.

While there are challenges and limitations in the use of ecological metrics with FTMS data, we show that there is a tangible path forward. In particular, our simulation model revealed good performance of some common ecological metrics of α-diversity, β-diversity, and functional trait values. We infer that conceptual and mechanistic inferences are likely to be valid when based on analyses such as comparing peak-intensity-based ecological metrics across experimental treatments or variation along environmental gradients. The performance of intensity-weighted mean trait values was particularly good in terms of both qualitative and quantitative aspects. We emphasize that we studied a small set of metrics and our inferences only extend to these metrics. Fortunately, it is straightforward to extend the simulation model to additional metrics (e.g., Hill numbers; Hill, 1973) and analyses (e.g., species abundance distributions; McGill et al., 2007). We suggest that users of FTMS data do this before applying abundance-based ecological metrics to real-world datasets. This will provide objective guidance on how to use (and whether to avoid) specific metrics for specific FTMS datasets.

To enable robust use of FTMS peak intensity data in future studies, we recommend use and further development of the simulation model developed here. The simulation model is the only tool we are aware of that can provide objective evaluations of uncertainty and potential biases associated with using FTMS peak intensities to compute ecological metrics. The model should not be taken as a static or mature tool, however. We encourage future work to expand it to include additional ecological metrics/analyses, situations with more than two samples, sample-to-sample variation in peak richness, links between peak richness and peak intensity, other ways of modeling error, and measured levels of error between concentrations and peak intensities. These evaluations are outside of the scope of this work, but will be straightforward to include in future versions of the simulation model. Such additions will allow each study to customize the model for their specific application. It should be possible to include the number of samples, the number of peaks in each sample, the peak intensity distributions, number of replicates, and the specific ecological analyses that will be applied. In turn, simulation model outcomes can provide objective guidance tailored to each study. One may think of the resulting guidance as akin to a power analysis whereby the simulation can indicate what can and cannot be inferred from a given dataset. For example, the model indicates that observed Bray-Curtis values have little to no correspondence to true values when Bray-Curtis is below ~0.2 (Fig. 10B, D). Bray-Curtis near and below ~0.2 are commonly observed in FTMS studies (e.g., Hawkes et al., 2016; Derrien et al., 2018; Bao et al., 2018), and this disconnect between observations and truth is maintained even with 1000 peaks per sample (Fig. 10D). In turn, FTMS studies that observe Bray-Curtis below ~0.2 may not be able to use those observations to make valid conceptual inferences. However, quantitative guidance must be developed for each study and we recommend that a version of the simulation model should be used by future studies using peak intensities to conduct ecological analyses of FTMS data. It may be that in time we understand the general rules well enough to leave the simulation behind, but for now, we suggest its use is warranted to ensure robust inferences.

In addition to further use and development of the simulation model, we recommend translation of other modeling approaches for use with FTMS data. Two potential approaches are based in machine learning and hierarchical modeling. Machine learning could be used to model the instrument response for a diverse chemical space in typical environmental samples to learn how measured signal intensities may relate to true concentrations. Even if such a model does not yield high-accuracy results, it may nonetheless help understand error/biases and provide additional guidance for robust use of peak intensity data. Potentially in concert with machine learning, hierarchical modeling could be translated from its application in ecological analyses (Iknayan et al., 2014) for use with FTMS. This approach has been used to model sources of error that lead to variation in detectability across biological species, such as variation in species visibility (e.g., Dorazio and Royle, 2005). In turn, data can essentially be corrected by accounting for the modeled sources of error (Roth et al., 2018), even revealing 'hidden diversity' (Richter et al., 2021). There are likely direct analogs to FTMS data in terms of variation among molecules in detectability due to variation in ionization and molecular interactions discussed in previous sections. Machine learning could be used to understand sources of error and, in turn, inform hierarchical models aimed at improving the mapping between peak intensity and concentration. If successful, this would increase the quality of information provided by peak intensities in both existing and future datasets.

In summary, FTMS has many strengths and weaknesses just like any analytical platform. Other types of compositional data also contain biases and uncertainties, such as the lack of true quantitation in sequence-based microbiome data (Gloor et al., 2017). Careful use of FTMS peak intensity data informed by objective, model-based guidance can overcome some of its weaknesses. We encourage further development of the model presented here and inclusion of additional methods developed to address issues that arise in similar data types (e.g., Gloor et al., 2017; Hardwick et al., 2018; Vieira-Silva et al., 2019). While these are important directions, we emphasize that despite peak intensities not necessarily reflecting concentrations, ecological metrics overall appear to perform well. This is likely due to the law of large numbers as FTMS, especially FTICR MS, datasets often contain 1000 or more peaks per sample. Our simulation results indicate that large numbers of identified peaks allow ecological metrics to essentially track towards their true values. We are encouraged by this outcome and look forward to further applications of ecological metrics, concepts, and theory to NOM chemistry.

7 Code Availability: R code for running the simulation models is available on GitHub: https://github.com/stegen/Peak_Intensity_Sims. Python code used to process the empirical data and to generate the associated figures will be available upon publication.

8 Data Availability: Raw and processed data will be made publicly available upon manuscript acceptance.

9 Author Contributions: WK contributed to conceptualization, experimental data curation, formal analysis, methodology, software, visualization, writing-original draft, writing-review/editing; AMP contributed to conceptualization, methodology, visualization, writing-original draft, writing-review/editing; CHC and SMC contributed to investigation and writing-review/editing; JE contributed to sample preparation and writing-review/editing; MMT contributed to conceptualization, methodology, writing-review/editing; JH contributed to conceptualization and writing-review/editing; RKC contributed to project administration, conceptualization, experimental data curation, methodology, writing-review/editing; JCS contributed to conceptualization, simulation data curation, formal analysis, funding acquisition, investigation, methodology, software, visualization, writing-original draft, writing-review/editing.

10 Competing interests: The authors declare that they have no conflict of interest.

11 Acknowledgements: A portion of this research was performed on a project award (doi:10.46936/intm.proj.2020.51667/60000248) from the Environmental Molecular Sciences Laboratory, a DOE Office of Science User Facility sponsored by the Biological and Environmental Research program under Contract No. DE-AC05-76RL01830. JCS was also supported by an Early Career Award (grant 74193) to JCS at Pacific Northwest National Laboratory (PNNL), a multiprogram national laboratory operated by Battelle for the United States Department of Energy under contract DE-AC05-76RL01830. We thank Alan Roebuck for useful feedback on the manuscript, Nathan Johnson for graphics development, Charles T. Resch for supplying the artificial river water, Patricia Miller and Jason Toyoda for lab support.

12 References

Anderson, M. J., Crist, T. O., Chase, J. M., Vellend, M., Inouye, B. D., Freestone, A. L., Sanders, N. J., Cornell, H. V., Comita, L. S., Davies, K. F., Harrison, S. P., Kraft, N. J. B., Stegen, J. C., and Swenson, N. G.: Navigating the multiple meanings of β diversity: a roadmap for the practicing ecologist, Ecol. Lett., 14, 19–28, https://doi.org/10.1111/j.1461-0248.2010.01552.x, 2011.

Bahureksa, W., Tfaily, M. M., Boiteau, R. M., Young, R. B., Logan, M. N., McKenna, A. M., and Borch, T.: Soil Organic Matter Characterization by Fourier Transform Ion Cyclotron Resonance Mass Spectrometry (FTICR MS): A Critical Review of Sample Preparation, Analysis, and Data Interpretation, Environ. Sci. Technol., 55, 9637–9656, https://doi.org/10.1021/acs.est.1c01135, 2021.

Bao, H., Niggemann, J., Luo, L., Dittmar, T., and Kao, S.-J.: Molecular composition and origin of water-soluble organic matter in marine aerosols in the Pacific off China, Atmos. Environ., 191, 27–35, https://doi.org/10.1016/j.atmosenv.2018.07.059, 2018.

Boye, K., Noël, V., Tfaily, M. M., Bone, S. E., Williams, K. H., Bargar, J. R., and Fendorf, S.: Thermodynamically controlled preservation of organic carbon in floodplains, Nat. Geosci., 10, 415–419, https://doi.org/10.1038/ngeo2940, 2017.

Cao, D., Lv, J., Geng, F., Rao, Z., Niu, H., Shi, Y., Cai, Y., and Kang, Y.: Ion Accumulation Time Dependent Molecular Characterization of Natural Organic Matter Using Electrospray Ionization-Fourier Transform Ion Cyclotron Resonance Mass Spectrometry, Anal. Chem., 88, 12210–12218, https://doi.org/10.1021/acs.analchem.6b03198, 2016.

Danczak, R. E., Chu, R. K., Fansler, S. J., Goldman, A. E., Graham, E. B., Tfaily, M. M., Toyoda, J., and Stegen, J. C.: Using metacommunity ecology to understand environmental metabolomes, Nat. Commun., 11, 6369, https://doi.org/10.1038/s41467-020-19989-y, 2020.

Danczak, R. E., Goldman, A. E., Chu, R. K., Toyoda, J. G., Garayburu-Caruso, V. A., Tolić, N., Graham, E. B., Morad, J. W., Renteria, L., Wells, J. R., Herzog, S. P., Ward, A. S., and Stegen, J. C.: Ecological theory applied to environmental metabolomes reveals compositional divergence despite conserved molecular properties, Sci. Total Environ., 788, 147409, https://doi.org/10.1016/j.scitotenv.2021.147409, 2021.

Derrien, M., Lee, Y. K., Shin, K.-H., and Hur, J.: Comparing discrimination capabilities of fluorescence spectroscopy versus FT-ICR-MS for sources and hydrophobicity of sediment organic matter, Environ. Sci. Pollut. Res., 25, 1892–1902, https://doi.org/10.1007/s11356-017-0531-z, 2018.

Dorazio, R. M. and Royle, J. A.: Estimating Size and Composition of Biological Communities by Modeling the Occurrence of Species, J. Am. Stat. Assoc., 100, 389–398, https://doi.org/10.1198/016214505000000015, 2005.

Elliott, K. J., Boring, L. R., Swank, W. T., and Haines, B. R.: Successional changes in plant species diversity and composition after clearcutting a Southern Appalachian watershed, For. Ecol. Manag., 92, 67–85, https://doi.org/10.1016/S0378-1127(96)03947-3, 1997.

Garayburu-Caruso, V. A., Stegen, J. C., Song, H.-S., Renteria, L., Wells, J., Garcia, W., Resch, C. T., Goldman, A. E., Chu, R. K., Toyoda, J., and Graham, E. B.: Carbon Limitation Leads to Thermodynamic Regulation of Aerobic Metabolism, Environ. Sci. Technol. Lett., 7, 517–524, https://doi.org/10.1021/acs.estlett.0c00258, 2020.

Gloor, G. B., Macklaim, J. M., Pawlowsky-Glahn, V., and Egozcue, J. J.: Microbiome Datasets Are Compositional: And This Is Not Optional, Front. Microbiol., 8, 2017.
Han, L., Kaesler, J., Peng, C., Reemtsma, T., and Lechtenfeld, O. J.: Online Counter Gradient LC-FT-ICR-MS Enables Detection of Highly Polar Natural Organic Matter Fractions, Anal. Chem., 93, 1740–1748, https://doi.org/10.1021/acs.analchem.0c04426, 2021.
Hardwick, S. A., Chen, W. Y., Wong, T., Kanakamedala, B. S., Deveson, I. W., Ongley, S. E., Santini, N. S., Marcellin, E., Smith, M. A., Nielsen, L. K., Lovelock, C. E., Neilan, B. A., and Mercer, T. R.: Synthetic microbe communities provide internal reference standards for metagenome sequencing and analysis, Nat. Commun., 9, 3096, https://doi.org/10.1038/s41467-018-05555-0, 2018.
Hawkes, J. A. and Kew, W.: 4 - High-resolution mass spectrometry strategies for the investigation of dissolved organic matter, in: Multidimensional Analytical Techniques in Environmental Research, edited by: Duarte, R. M. B. O. and Duarte, A. C., Elsevier, 71–104, https://doi.org/10.1016/B978-0-12-818896-5.00004-1, 2020a.
Hawkes, J. A. and Kew, W.: 4 - High-resolution mass spectrometry strategies for the investigation of dissolved organic matter, in: Multidimensional Analytical Techniques in Environmental Research, edited by: Duarte, R. M. B. O. and Duarte, A. C., Elsevier, 71–104, https://doi.org/10.1016/B978-0-12-818896-5.00004-1, 2020b.
Hawkes, J. A., Dittmar, T., Patriarca, C., Tranvik, L., and Bergquist, J.: Evaluation of the Orbitrap Mass Spectrometer for the Molecular Fingerprinting Analysis of Natural Dissolved Organic Matter, Anal. Chem., 88, 7698–7704, https://doi.org/10.1021/acs.analchem.6b01624, 2016.
Hedges, J. I., Eglinton, G., Hatcher, P. G., Kirchman, D. L., Arnosti, C., Derenne, S., Evershed, R. P., Kögel-Knabner, I., de Leeuw, J. W., Littke, R., Michaelis, W., and Rullkötter, J.: The molecularly-uncharacterized component of nonliving organic matter in natural environments, Org. Geochem., 31, 945–958, https://doi.org/10.1016/S0146-6380(00)00096-6, 2000.
Hill, M. O.: Diversity and Evenness: A Unifying Notation and Its Consequences, Ecology, 54, 427–432, https://doi.org/10.2307/1934352, 1973.
Iknayan, K. J., Tingley, M. W., Furnas, B. J., and Beissinger, S. R.: Detecting diversity: emerging methods to estimate species diversity, Trends Ecol. Evol., 29, 97–106, https://doi.org/10.1016/j.tree.2013.10.012, 2014.
Kaiser, N. K., McKenna, A. M., Savory, J. J., Hendrickson, C. L., and Marshall, A. G.: Tailored Ion Radius Distribution for Increased Dynamic Range in FT-ICR Mass Analysis of Complex Mixtures, Anal. Chem., 85, 265–272, https://doi.org/10.1021/ac302678v, 2013.
Kellerman, A. M., Dittmar, T., Kothawala, D. N., and Tranvik, L. J.: Chemodiversity of dissolved organic matter in lakes driven by climate and hydrology, Nat. Commun., 5, 3804, https://doi.org/10.1038/ncomms4804, 2014.
Kim, D., Kim, S., Son, S., Jung, M.-J., and Kim, S.: Application of Online Liquid Chromatography 7 T FT-ICR Mass Spectrometer Equipped with Quadrupolar Detection for Analysis of Natural Organic Matter, Anal. Chem., 91, 7690–7697, https://doi.org/10.1021/acs.analchem.9b00689, 2019.
Kruve, A.: Strategies for Drawing Quantitative Conclusions from Nontargeted Liquid Chromatography–High-Resolution Mass Spectrometry Analysis, Anal. Chem., 92, 4691–4699, https://doi.org/10.1021/acs.analchem.9b03481, 2020.
Kruve, A., Kaupmees, K., Liigand, J., and Leito, I.: Negative Electrospray Ionization via Deprotonation: Predicting the Ionization Efficiency, Anal. Chem., 86, 4822–4830, https://doi.org/10.1021/ac404066v, 2014.
Kujawinski, E. B.: Electrospray Ionization Fourier Transform Ion Cyclotron Resonance Mass Spectrometry (ESI FT-ICR MS): Characterization of Complex Environmental Mixtures, Environ. Forensics, 3, 207–216, https://doi.org/10.1006/enfo.2002.0109, 2002.
Kujawinski, E. B., Longnecker, K., Blough, N. V., Vecchio, R. D., Finlay, L., Kitner, J. B., and Giovannoni, S. J.: Identification of possible source markers in marine dissolved organic matter using ultrahigh resolution mass spectrometry, Geochim. Cosmochim. Acta, 73, 4384–4399, https://doi.org/10.1016/j.gca.2009.04.033, 2009.

LaRowe, D. E. and Van Cappellen, P.: Degradation of natural organic matter: A thermodynamic analysis, Geochim. Cosmochim. Acta, 75, 2030–2042, https://doi.org/10.1016/j.gca.2011.01.020, 2011.
Leyva, D., Tose, L. V., Porter, J., Wolff, J., Jaffé, R., and Fernandez-Lima, F.: Understanding the structural complexity of dissolved organic matter: isomeric diversity, Faraday Discuss., 218, 431–440, https://doi.org/10.1039/C8FD00221E, 2019.
Leyva, D., Jaffe, R., and Fernandez-Lima, F.: Structural Characterization of Dissolved Organic Matter at the Chemical Formula Level Using TIMS-FT-ICR MS/MS, Anal. Chem., 92, 11960–11966, https://doi.org/10.1021/acs.analchem.0c02347, 2020.
Li, H.-Y., Wang, H., Wang, H.-T., Xin, P.-Y., Xu, X.-H., Ma, Y., Liu, W.-P., Teng, C.-Y., Jiang, C.-L., Lou, L.-P., Arnold, W., Cralle, L., Zhu, Y.-G., Chu, J.-F., Gilbert, J. A., and Zhang, Z.-J.: The chemodiversity of paddy soil dissolved organic matter correlates with microbial community at continental scales, Microbiome, 6, 187, https://doi.org/10.1186/s40168-018-0561-x, 2018.
Li, Y., Harir, M., Uhl, J., Kanawati, B., Lucio, M., Smirnov, K. S., Koch, B. P., Schmitt-Kopplin, P., and Hertkorn, N.: How representative are dissolved organic matter (DOM) extracts? A comprehensive study of sorbent selectivity for DOM isolation, Water Res., 116, 316–323, https://doi.org/10.1016/j.watres.2017.03.038, 2017.
Lucas, J., Koester, I., Wichels, A., Niggemann, J., Dittmar, T., Callies, U., Wiltshire, K. H., and Gerdts, G.: Short-Term Dynamics of North Sea Bacterioplankton-Dissolved Organic Matter Coherence on Molecular Level, Front. Microbiol., 7, 2016.
Makarov, A., Denisov, E., Kholomeev, A., Balschun, W., Lange, O., Strupat, K., and Horning, S.: Performance Evaluation of a Hybrid Linear Ion Trap/Orbitrap Mass Spectrometer, Anal. Chem., 78, 2113–2120, https://doi.org/10.1021/ac0518811, 2006.
Makarov, A., Grinfeld, D., and Ayzikov, K.: Chapter 2 - Fundamentals of Orbitrap analyzer, in: Fundamentals and Applications of Fourier Transform Mass Spectrometry, edited by: Kanawati, B. and Schmitt-Kopplin, P., Elsevier, 37–61, https://doi.org/10.1016/B978-0-12-814013-0.00002-8, 2019.
Marshall, A. G., Hendrickson, C. L., and Jackson, G. S.: Fourier transform ion cyclotron resonance mass spectrometry: A primer, Mass Spectrom. Rev., 17, 1–35, https://doi.org/10.1002/(SICI)1098-2787(1998)17:1<1::AID-MAS1>3.0.CO;2-K, 1998.
McGill, B. J., Etienne, R. S., Gray, J. S., Alonso, D., Anderson, M. J., Benecha, H. K., Dornelas, M., Enquist, B. J., Green, J. L., He, F., Hurlbert, A. H., Magurran, A. E., Marquet, P. A., Maurer, B. A., Ostling, A., Soykan, C. U., Ugland, K. I., and White, E. P.: Species abundance distributions: moving beyond single prediction theories to integration within an ecological framework, Ecol. Lett., 10, 995–1015, https://doi.org/10.1111/j.1461-0248.2007.01094.x, 2007.
Merder, J., Röder, H., Dittmar, T., Feudel, U., Freund, J. A., Gerdts, G., Kraberg, A., and Niggemann, J.: Dissolved organic compounds with synchronous dynamics share chemical properties and origin, Limnol. Oceanogr., n/a, https://doi.org/10.1002/lno.11938, 2021.
Mouillot, D. and Leprêtre, A.: A comparison of species diversity estimators, Res. Popul. Ecol., 41, 203–215, https://doi.org/10.1007/s101440050024, 1999.
Muscarella, R. and Uriarte, M.: Do community-weighted mean functional traits reflect optimal strategies?, Proc. R. Soc. B Biol. Sci., 283, 20152434, https://doi.org/10.1098/rspb.2015.2434, 2016.
Osterholz, H., Singer, G., Wemheuer, B., Daniel, R., Simon, M., Niggemann, J., and Dittmar, T.: Deciphering associations between dissolved organic molecules and bacterial communities in a pelagic marine system, ISME J., 10, 1717–1730, https://doi.org/10.1038/ismej.2015.231, 2016.
Raeke, J., Lechtenfeld, O. J., Wagner, M., Herzsprung, P., and Reemtsma, T.: Selectivity of solid phase extraction of freshwater dissolved organic matter and its effect on ultrahigh resolution mass spectra, Environ. Sci. Process. Impacts, 18, 918–927, https://doi.org/10.1039/C6EM00200E, 2016.
Redowan, M.: Spatial pattern of tree diversity and evenness across forest types in Majella National Park, Italy, For. Ecosyst., 2, 24, https://doi.org/10.1186/s40663-015-0048-1, 2015.
Richter, A., Nakamura, G., Agra Iserhard, C., and da Silva Duarte, L.: The hidden side of diversity: Effects of imperfect detection on multiple dimensions of biodiversity, Ecol. Evol., 11, 12508–12519,

https://doi.org/10.1002/ece3.7995, 2021.
Roth, T., Allan, E., Pearman, P. B., and Amrhein, V.: Functional ecology and imperfect detection of species, Methods Ecol. Evol., 9, 917–928, https://doi.org/10.1111/2041-210X.12950, 2018.
Roth, V.-N., Lange, M., Simon, C., Hertkorn, N., Bucher, S., Goodall, T., Griffiths, R. I., Mellado-Vázquez, P. G., Mommer, L., Oram, N. J., Weigelt, A., Dittmar, T., and Gleixner, G.: Persistence of dissolved organic matter explained by molecular changes during its passage through soil, Nat. Geosci., 12, 755–761, https://doi.org/10.1038/s41561-019-0417-4, 2019.
Ruddy, B. M., Hendrickson, C. L., Rodgers, R. P., and Marshall, A. G.: Positive Ion Electrospray Ionization Suppression in Petroleum and Complex Mixtures, Energy Fuels, 32, 2901–2907, https://doi.org/10.1021/acs.energyfuels.7b03204, 2018.
Senko, M. W., Hendrickson, C. L., Emmett, M. R., Shi, S. D.-H., and Marshall, A. G.: External Accumulation of Ions for Enhanced Electrospray Ionization Fourier Transform Ion Cyclotron Resonance Mass Spectrometry, J. Am. Soc. Mass Spectrom., 8, 970–976, https://doi.org/10.1016/S1044-0305(97)00126-8, 1997.
Shaw, J. B., Lin, T.-Y., Leach, F. E., Tolmachev, A. V., Tolić, N., Robinson, E. W., Koppenaal, D. W., and Paša-Tolić, L.: 21 Tesla Fourier Transform Ion Cyclotron Resonance Mass Spectrometer Greatly Expands Mass Spectrometry Toolbox, J. Am. Soc. Mass Spectrom., 27, 1929–1936, https://doi.org/10.1007/s13361-016-1507-9, 2016.
Smith, D. F., Podgorski, D. C., Rodgers, R. P., Blakney, G. T., and Hendrickson, C. L.: 21 Tesla FT-ICR Mass Spectrometer for Ultrahigh-Resolution Analysis of Complex Organic Mixtures, Anal. Chem., 90, 2041–2047, https://doi.org/10.1021/acs.analchem.7b04159, 2018.
Steen, A. D., Kusch, S., Abdulla, H. A., Cakić, N., Coffinet, S., Dittmar, T., Fulton, J. M., Galy, V., Hinrichs, K.-U., Ingalls, A. E., Koch, B. P., Kujawinski, E., Liu, Z., Osterholz, H., Rush, D., Seidel, M., Sepúlveda, J., and Wakeham, S. G.: Analytical and Computational Advances, Opportunities, and Challenges in Marine Organic Biogeochemistry in an Era of "Omics," Front. Mar. Sci., 7, 2020.
Tanentzap, A. J., Fitch, A., Orland, C., Emilson, E. J. S., Yakimovich, K. M., Osterholz, H., and Dittmar, T.: Chemical and microbial diversity covary in fresh water to influence ecosystem functioning, Proc. Natl. Acad. Sci., 116, 24689–24695, https://doi.org/10.1073/pnas.1904896116, 2019.
Tose, L. V., Benigni, P., Leyva, D., Sundberg, A., Ramírez, C. E., Ridgeway, M. E., Park, M. A., Romão, W., Jaffé, R., and Fernandez-Lima, F.: Coupling trapped ion mobility spectrometry to mass spectrometry: trapped ion mobility spectrometry–time-of-flight mass spectrometry versus trapped ion mobility spectrometry–Fourier transform ion cyclotron resonance mass spectrometry, Rapid Commun. Mass Spectrom., 32, 1287–1295, https://doi.org/10.1002/rcm.8165, 2018.
Trufelli, H., Palma, P., Famiglini, G., and Cappiello, A.: An overview of matrix effects in liquid chromatography–mass spectrometry, Mass Spectrom. Rev., 30, 491–509, https://doi.org/10.1002/mas.20298, 2011.
Urban, P. L.: Quantitative mass spectrometry: an overview, Philos. Trans. R. Soc. Math. Phys. Eng. Sci., 374, 20150382, https://doi.org/10.1098/rsta.2015.0382, 2016.
Vieira-Silva, S., Sabino, J., Valles-Colomer, M., Falony, G., Kathagen, G., Caenepeel, C., Cleynen, I., van der Merwe, S., Vermeire, S., and Raes, J.: Quantitative microbiome profiling disentangles inflammation- and bile duct obstruction-associated microbiota alterations across PSC/IBD diagnoses, Nat. Microbiol., 4, 1826–1831, https://doi.org/10.1038/s41564-019-0483-9, 2019.
Wen, Z., Shang, Y., Lyu, L., Liu, G., Hou, J., He, C., Shi, Q., He, D., and Song, K.: Sources and composition of riverine dissolved organic matter to marginal seas from mainland China, J. Hydrol., 127152, https://doi.org/10.1016/j.jhydrol.2021.127152, 2021.
Whittaker, R. H.: Evolution and Measurement of Species Diversity, TAXON, 21, 213–251, https://doi.org/10.2307/1218190, 1972.
Wörner, T. P., Snijder, J., Bennett, A., Agbandje-McKenna, M., Makarov, A. A., and Heck, A. J. R.: Resolving heterogeneous macromolecular assemblies by Orbitrap-based single-particle charge detection mass spectrometry, Nat. Methods, 17, 395–398, https://doi.org/10.1038/s41592-020-0770-7, 2020.

Zark, M., Christoffers, J., and Dittmar, T.: Molecular properties of deep-sea dissolved organic matter are predictable by the central limit theorem: Evidence from tandem FT-ICR-MS, Mar. Chem., 191, 9–15, https://doi.org/10.1016/j.marchem.2017.02.005, 2017.

Figures

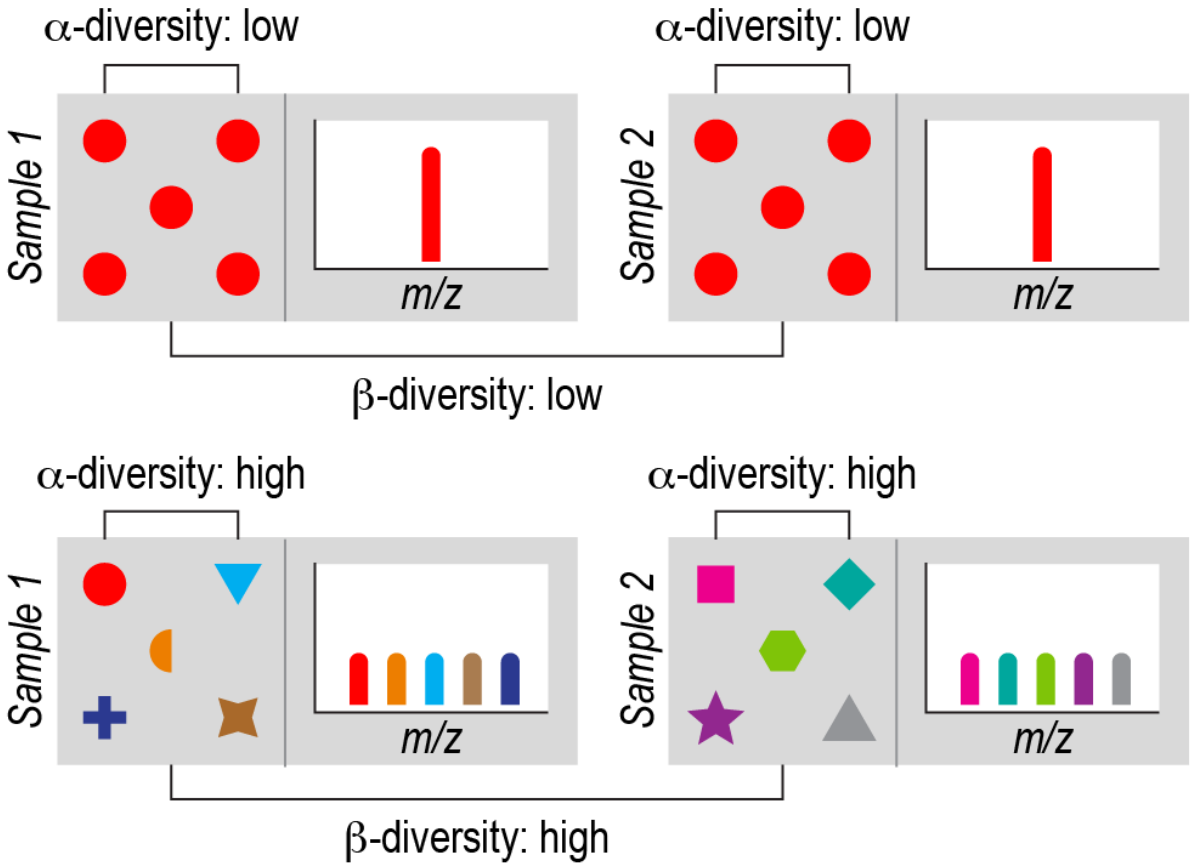

Figure 1. Ecological concepts of α-diversity and β-diversity. Each gray box represents a sample of an ecological community or collection of organic molecules (i.e., an OM assemblage). Symbols represent individual organisms or molecules. Different biological or molecular species are represented by a combination of shape and color. (Top) Each sample has one biological species (red circles) or one chemical species (red bar), and the species are the same within and between the samples. This reflects minimal α-diversity because there is a single species. This also reflects minimal β-diversity because there is no difference in which species are present in each sample. (Bottom) Each sample has five species (biological or chemical) represented by different colors and symbols. There are no shared species between samples. This reflects maximum α-diversity because every individual is a different species within each sample, and maximum β-diversity because there are no species shared between samples. In real ecological and OM samples, α-diversity and β-diversity fall between these extremes.

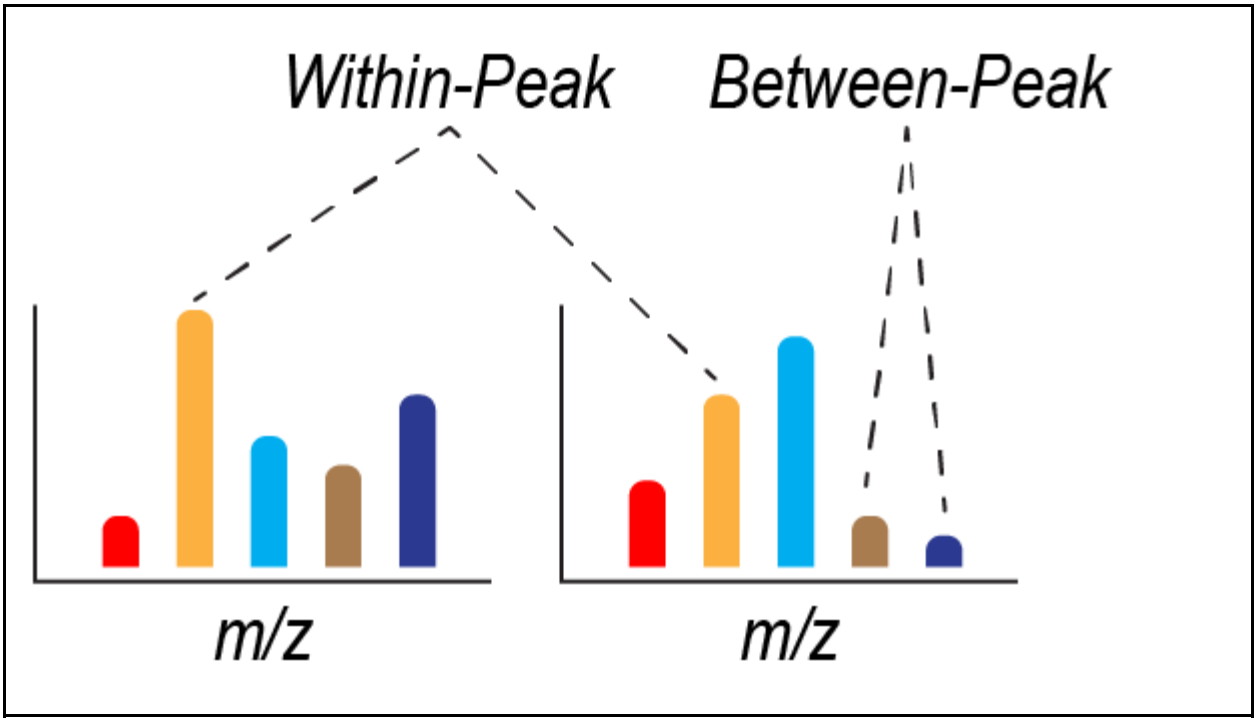

Figure 2. Summary of within-peak and between-peak comparisons of peak intensity. Two idealized mass spectra (i.e., from two samples) are shown with each peak defined by a mass-to-charge ratio (*m/z*) and represented by a different color. The intensity of each peak in each sample is represented by the height of each colored bar. Within-peak comparisons of intensity are based on comparing intensities at the same *m/z* across two or more samples. Between-peak comparisons of intensity are based on comparing intensities at two or more *m/z* values. Between-peak comparisons can be done within a sample (as shown) or between samples (not shown).

671

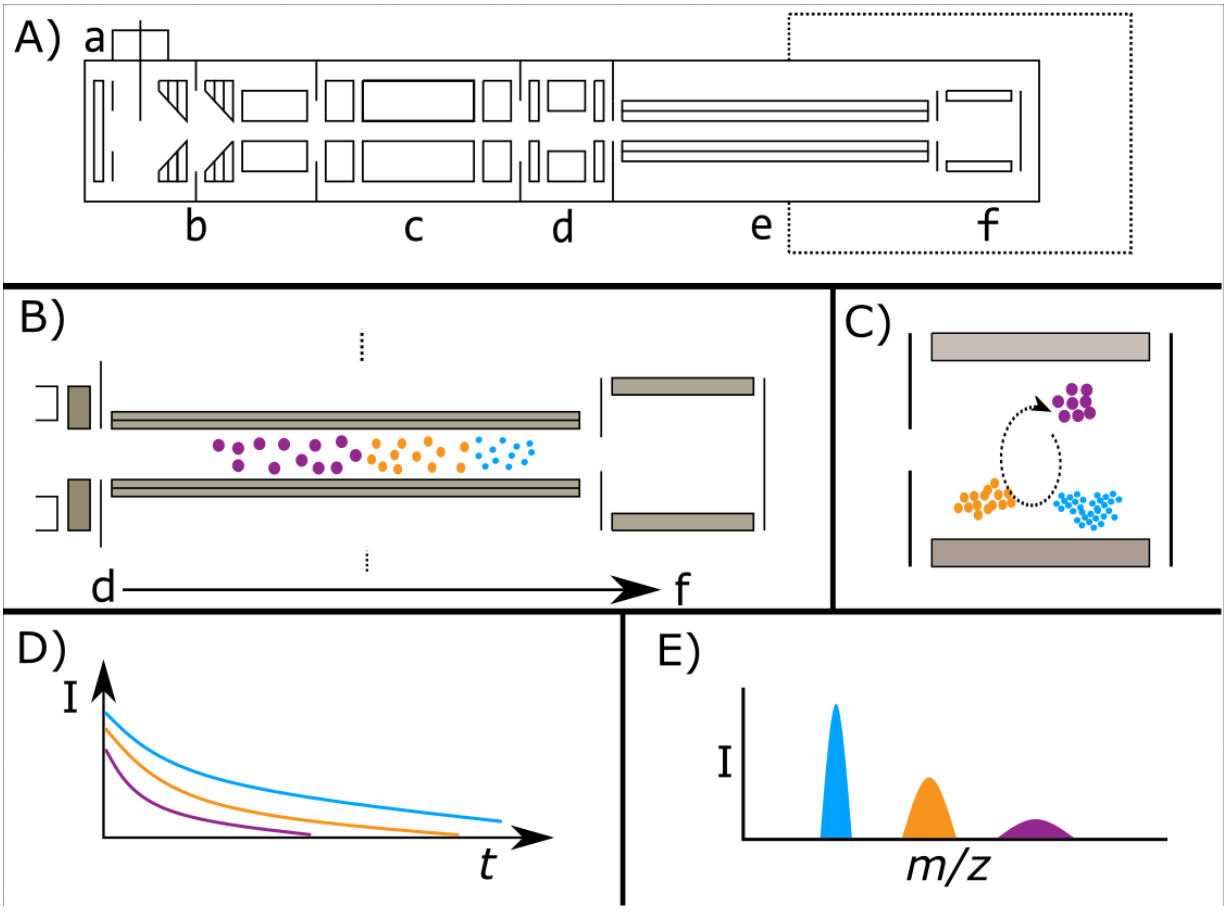

Figure 3. Illustrative example of a generic FTICR mass spectrometer (panel A), showing common and key biases between FTICR signal intensity and *m/z* of ions (B-E). Panel A shows the major elements of a generic FTICR mass spectrometer (based loosely on a Bruker solariX FTICR MS geometry). Panel A elements include; a - atmospheric pressure ionization source (i.e. ESI source), b - source ion optics (i.e. dual ion funnels), c - mass selecting quadrupole, d - collision cell, e - transfer multipoles to ICR cell, f - ICR cell. Dashed line indicates the magnetic field. Note: diagram is deliberately simplified and not to scale. Panel B) demonstrates the time-of-flight bias along the transfer multipoles (e) in the 'flight tube', from the collision cell (d) to the ICR cell (f). Lower *m/z* ions travel faster, as indicated by the smaller icons reaching the ICR cell first. Ions are shaded to aid visualization. Panel C) visualizes the effect of a variable excitation radii for ions of different masses, as may happen with a CHIRP excitation pulse. Lower *m/z* ions are closer to the detection electrodes (shaded in gray) and therefore will induce a larger image current. Note also the ion populations have been adjusted from B) to indicate biases from the time-of-flight effect. Panel D) shows the time-domain recorded signal intensity against time, with the ions having an initial intensity roughly proportional to the number of ions in that cloud. However, as time progresses the less abundant ion clouds lose coherence and destabilize more rapidly, resulting in an attenuation of their signal. Note that the real signal would follow a damped sinusoidal function; here an absolute value approximation is shown for simplicity. Panel E) shows the mass spectrum post-Fourier transform, demonstrating that the impact is not only on intensity (peak height), but also resolution (peak width). In all cases, effects are deliberately exaggerated and not-to-scale to aid interpretation.

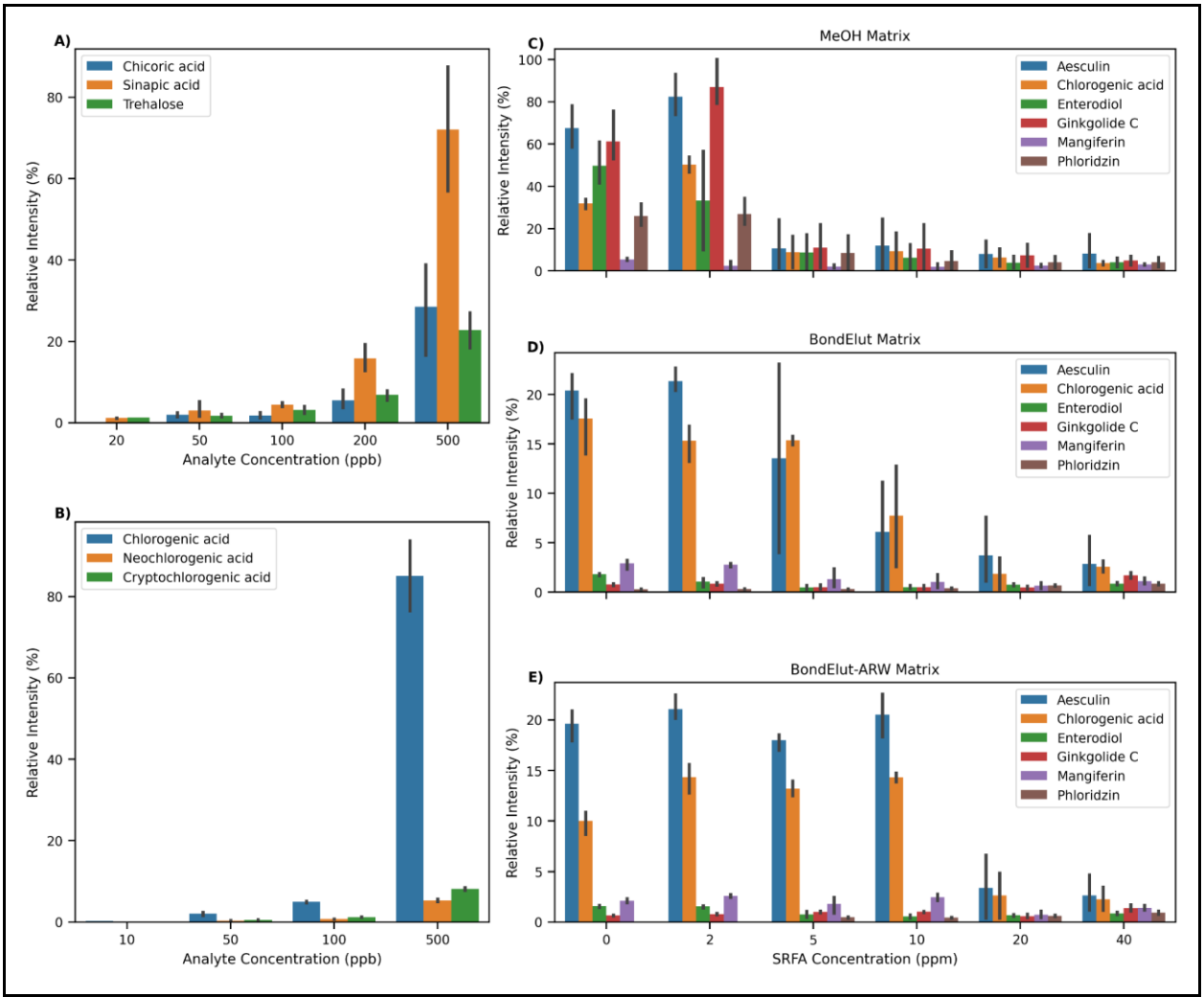

Figure 4 - A) Barplot visualization of the relationship between signal intensity (relative intensity) and concentration of analyte for three chemically distinct molecules analyzed contemporaneously but independently in pure methanol solvent. Relative intensity indicates data were scaled to the largest signal in any replicate from the associated series of spectra. Replicates are combined to show their mean and 95% confidence interval. B) As with A), but for three structural isomers of chlorogenic acid. C-E) Compounds spiked into three different solvent matrices (methanol, BondElut methanol, and BondElut artificial river water (ARW)) at a fixed concentration (100 ppb), but with addition of SRFA at varying concentrations from 0 to 40 ppm. In all cases, [M-H]- ion only is shown, but other ions (i.e. [M+Cl]-) were detected. 95% confidence intervals represent the results of triplicate measurements. Intensities have been scaled per plot for A and B, and are on the same scale for C-E).

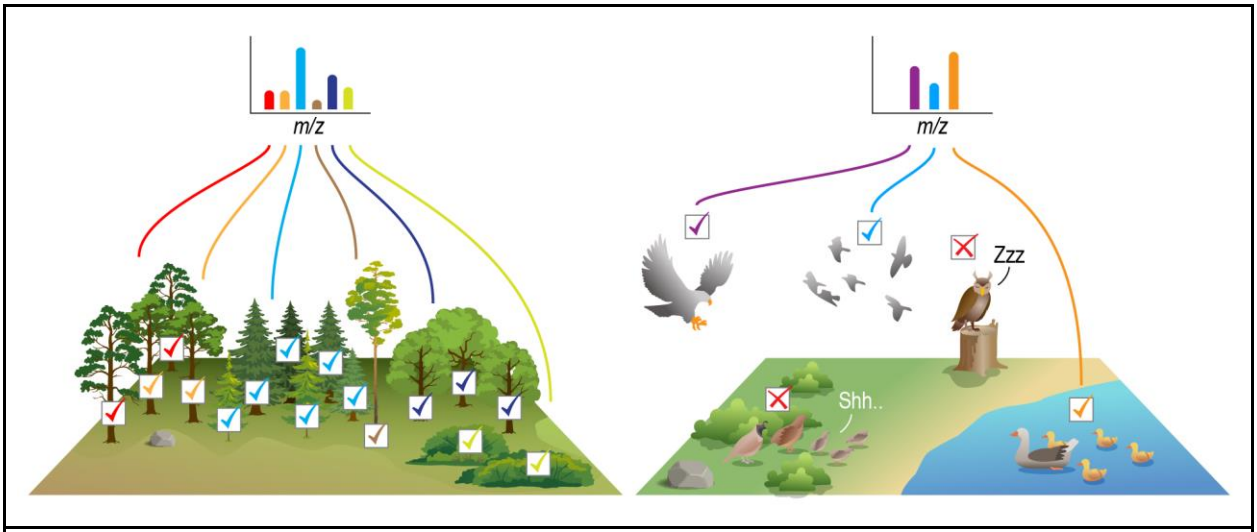

Figure 5. Graphical summary of how FTMS peak intensity data are often treated (left), which is distinct from the reality of those data (right). When surveying the number of individuals of each species within a tree community, there is good confidence that the measured abundances are close to real abundances. This is because there is relatively little variation across species in the ability to detect individuals. FTMS peak intensity data are often used as though they are like tree-community data. However, FTMS data are more like bird-community data. That is, the ability to detect different species varies due to intrinsic factors (e.g., activity patterns, how loud and often birds call, etc.) and extrinsic factors (e.g., habitat structural complexity, predator-induced behavioral changes, etc.). Similarly, the intrinsic physics of a given molecule will impact its ability to ionize and thus its observed peak intensity, and in environmental samples there are thousands of molecular species that impact the ionization 'behavior' of each other. FTMS data being more bird-like than tree-like needs to be accounted for when performing ecological analyses using FTMS data.

675

676

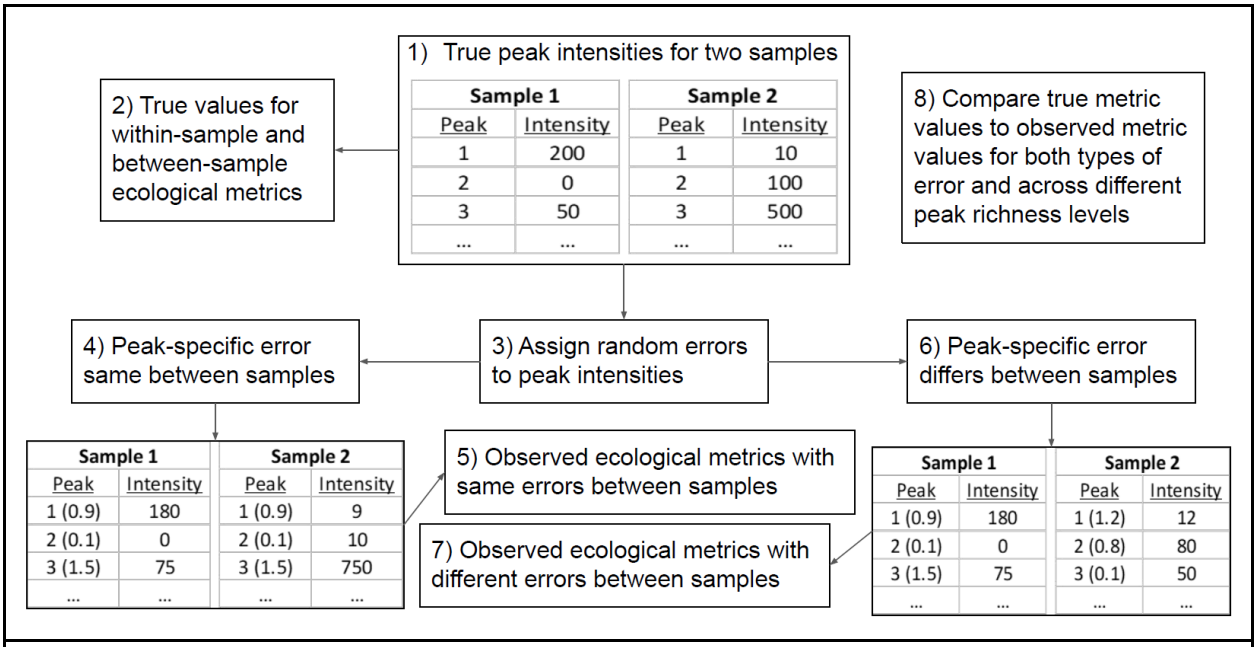

Figure 6. Flow diagram for the *in silico* simulation model. The model was used to evaluate how ecological metrics are impacted by variation in ionization across organic molecules (i.e., peaks). The true peak intensities are what is expected if intensity is linearly to concentration, and all peaks fall along the same linear function. Variation in ionization adds error around this idealized linear relationship. The error is modeled in two ways: the error applied to a given peak is either the same between samples (i.e., there are no variable matrix effects on ionization) or varies randomly between samples (i.e., there are variable matrix effects on ionization). In the lower tables the proportional error applied to each peak is provided parenthetically. The tables are for demonstration and show only three peaks per sample. The number of peaks per sample was set to either 100 or 1000.

677

678

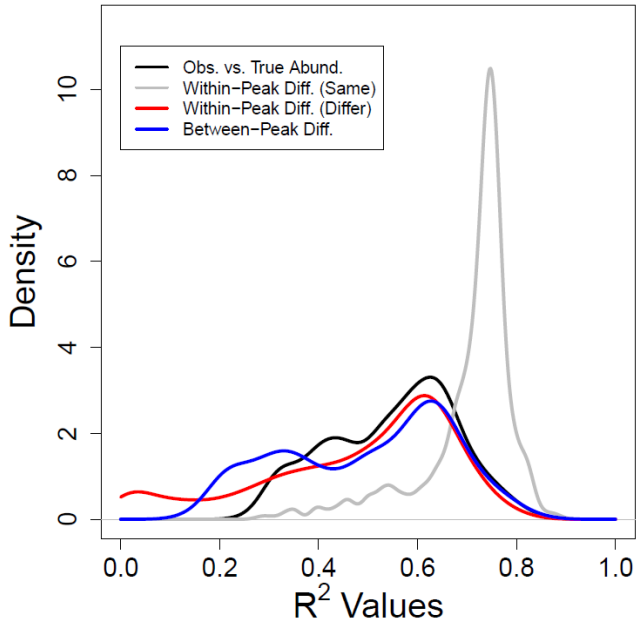

Figure 7. Variation in observed intensity explained by true abundance. Kernel density functions are shown for different relationships and types of error. Density functions were fit using R^2 values collated from across simulation iterations. Higher R^2 values indicate a stronger link (i.e., lower uncertainty) between observed intensities and true abundances. Black is for the relationship shown in Figure S1. Blue is for between-peak within-sample differences (example relationships shown in Figures 8A,B). Gray is for within-peak between-sample differences when the same peak-level error was used for both synthetic samples within a given simulation iteration (example relationship shown in Figure 8C). Red is for within-peak between-sample differences when different peak-level error was used across the synthetic samples within a given simulation iteration (example relationship shown in Figure 8D). While there are central tendencies in all four distributions, there is also significant variation in the degree to which observed intensities reflect true abundances.

679

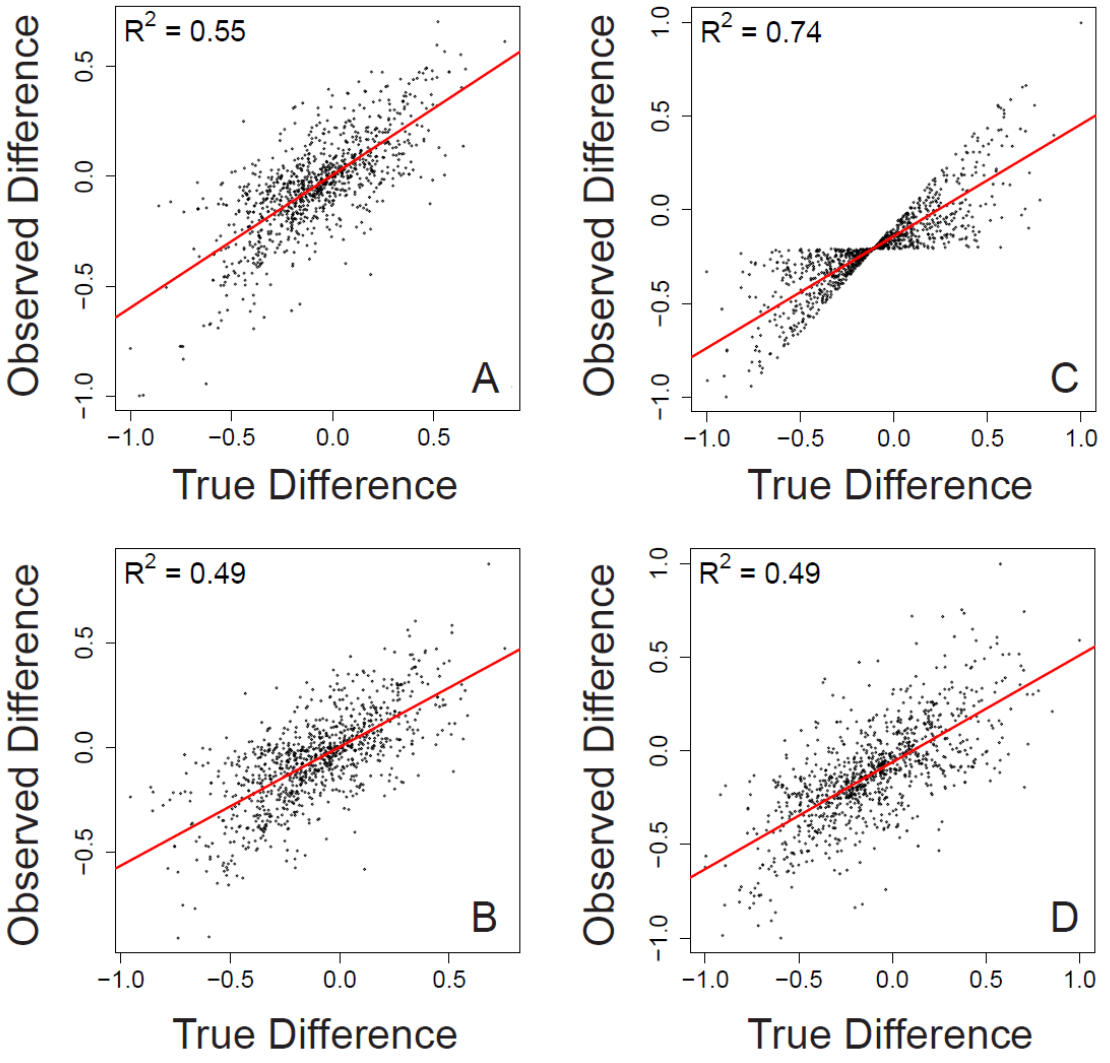

Figure 8. Observed differences in peak intensity as a function of true differences in peak intensity across both within-peak and between-peak comparisons and across both kinds of error. (A) Between-peak differences with the same error applied to a given peak between samples. (B) Between-peak differences with different errors applied to a given peak between samples. (C) Within-peak differences with the same error applied to a given peak between samples. (D) Within-peak differences with different errors applied to a given peak between samples. On all panels the red line represents the linear regression model, and the associated R^2 value is provided.

680

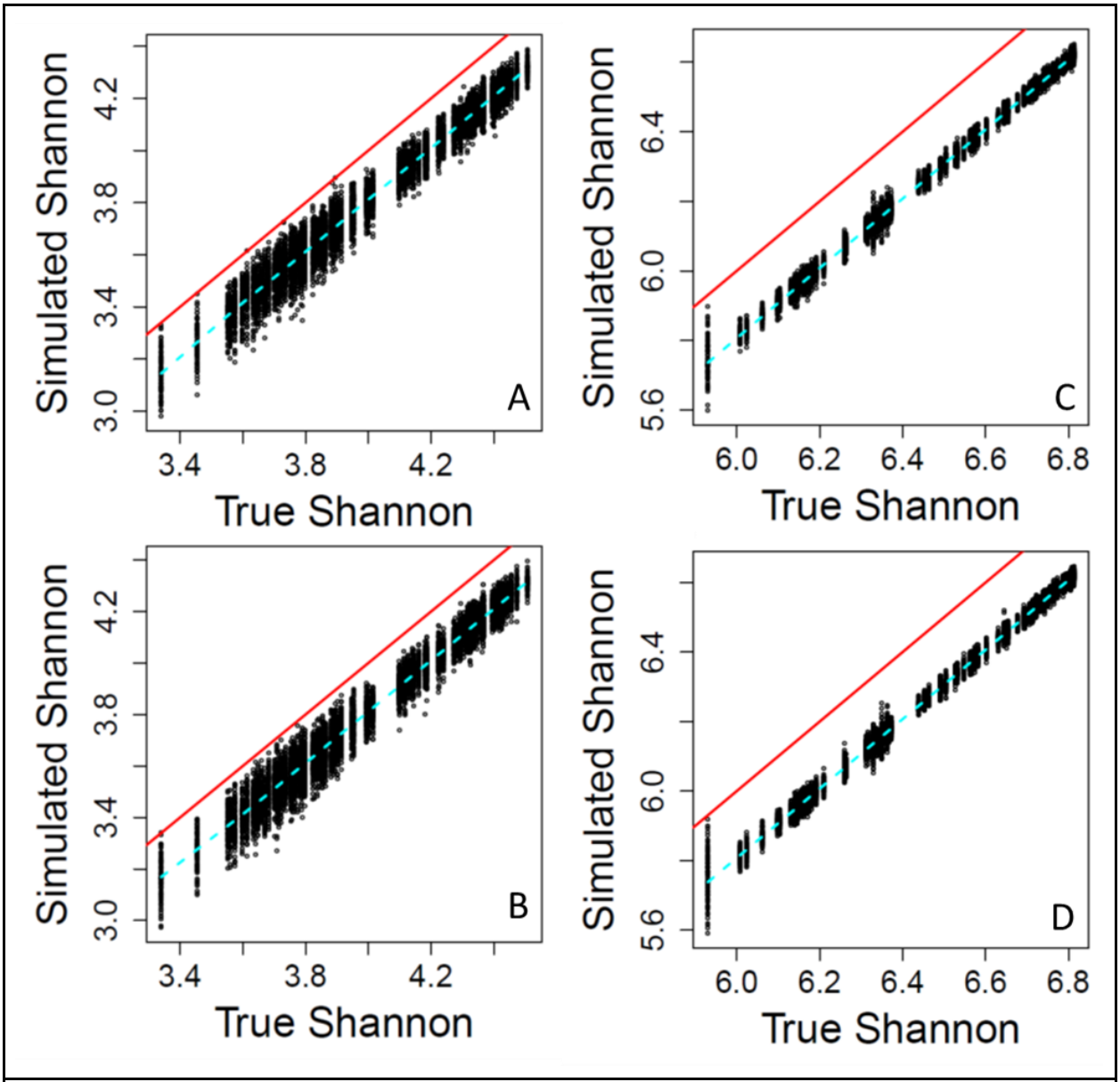

Figure 9. Shannon α-diversity that includes simulated error regressed against true Shannon, across different scenarios. (A) The same error applied to a given peak between samples, and 100 peaks per sample. (B) Different errors applied to a given peak between samples, and 100 peaks per sample. (C) The same error applied to a given peak between samples, and 1000 peaks per sample. (D) Different errors applied to a given peak between samples, and 1000 peaks per sample. On all panels the red line represents the one-to-one line and the dashed line is a spline fit to the data. All data are from the simulation model.

681

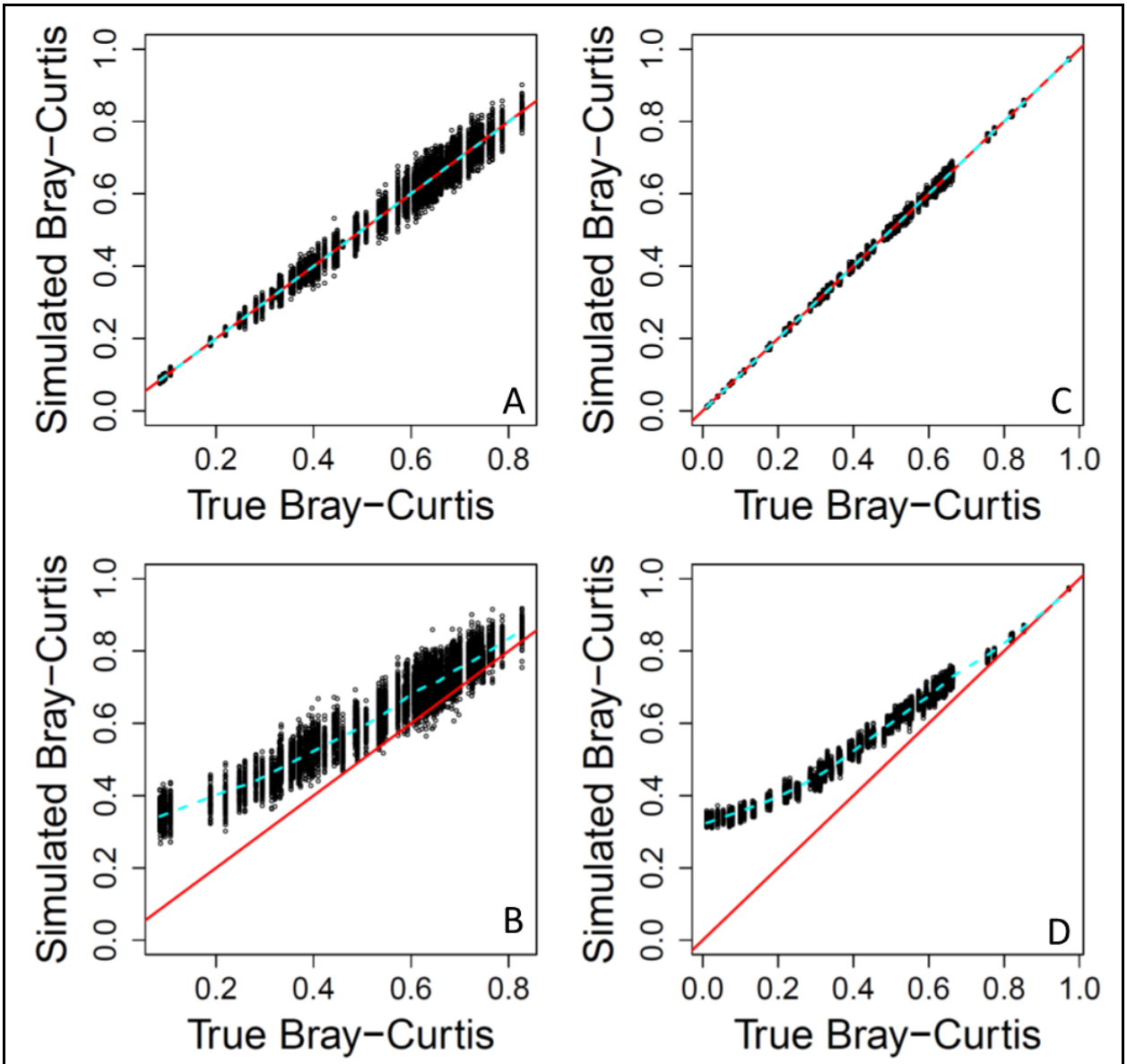

Figure 10. Bray-Curtis dissimilarity as a measure of β-diversity that includes simulated error regressed against true Bray-Curtis, across different scenarios. (A) The same error applied to a given peak between samples, and 100 peaks per sample. (B) Different errors applied to a given peak between samples, and 100 peaks per sample. (C) The same error applied to a given peak between samples, and 1000 peaks per sample. (D) Different errors applied to a given peak between samples, and 1000 peaks per sample. On all panels the red line represents the one-to-one line and the dashed line is a spline fit to the data. All data are from the simulation model.

682

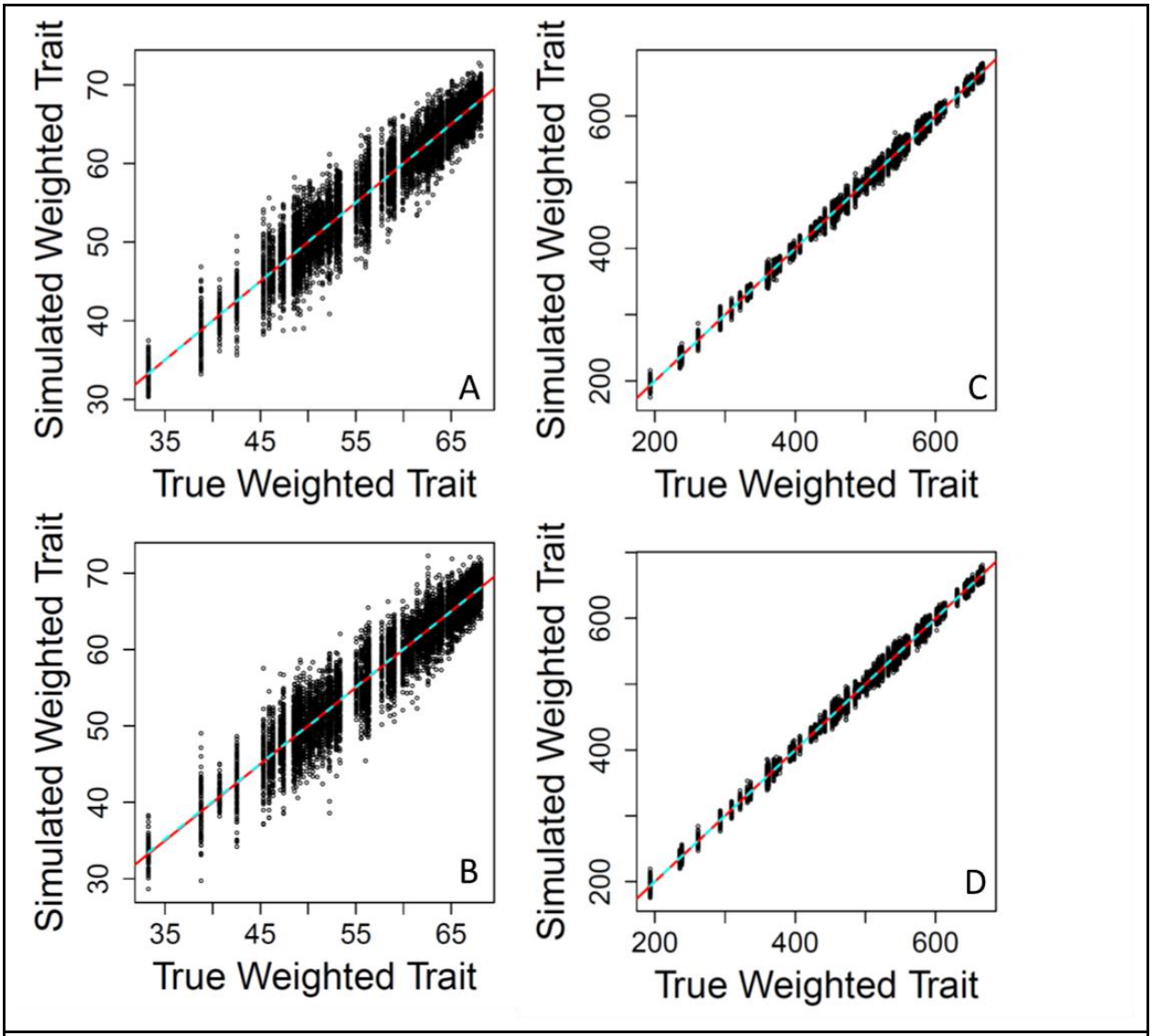

Figure 11. Mean peak-intensity-weighted trait values that include simulated error regressed against true mean peak-intensity-weighted trait values, across different scenarios. (A) The same error applied to a given peak between samples, and 100 peaks per sample. (B) Different errors applied to a given peak between samples, and 100 peaks per sample. (C) The same error applied to a given peak between samples, and 1000 peaks per sample. (D) Different errors applied to a given peak between samples, and 1000 peaks per sample. On all panels the red line represents the one-to-one line and the dashed line is a spline fit to the data. All data are from the simulation model.

683